



CO₂ emissions from peat-draining rivers regulated by water pH

Alexandra Klemme¹, Tim Rixen^{2,3}, Denise Müller-Dum¹, Moritz Müller⁴, Justus Notholt¹, and Thorsten Warneke¹

¹Institute of Environmental Physics, University of Bremen, Otto-Hahn-Allee 1, 28359 Bremen, Germany

²Leibniz Center for Tropical Marine Research, Fahrenheitstr. 6, 28359 Bremen, Germany

³Institute of Geology, University of Hamburg, Bundesstr. 55, 20146 Hamburg, Germany

⁴Faculty of Engineering, Computing, and Science, Swinburne University of Technology Sarawak Campus, Jalan Simpang Tiga, 93350 Kuching, Sarawak, Malaysia

Correspondence: Alexandra Klemme (aklemme@uni-bremen.de)

Abstract. Southeast Asian peatlands represent a globally significant carbon store that is destabilized by deforestation and the transformation into plantations, causing high carbon dioxide (CO₂) emissions from peat soils and increased leaching rates of peat carbon into rivers. While global model studies assumed that CO₂ emissions from peat-draining rivers would be high, estimates based on field data suggest they are only moderate. In this study we offer an explanation for this phenomenon and show that carbon decomposition is hampered by the low pH in peat-draining rivers, which limits CO₂ production in and emissions from these rivers. We find an exponential pH limitation that shows good agreement with laboratory measurements from high latitude peat soils. Additionally, our results suggest that enhanced input of carbonate minerals increase CO₂ emissions from peat-draining rivers by counteracting the pH limitation. As such inputs of carbonate minerals occur due to human activities like deforestation of river catchments, liming in plantations and enhanced weathering projects, our study points out an important feedback mechanism of those practices.

1 Introduction

Rivers and streams emit high amounts of carbon dioxide (CO₂) to the atmosphere (Cole et al., 2007), but estimates of these emissions (0.6 – 1.8 PgC yr⁻¹) are highly uncertain (Aufdenkampe et al., 2011; Raymond et al., 2013). Studies agree that more than three-quarters of the global river CO₂ emissions occur in the tropics (Raymond et al., 2013; Lauerwald et al., 2015). River CO₂ emissions are controlled by the partial pressure difference between CO₂ in the atmosphere and in the river water (Raymond et al., 2012), whereby riverine CO₂ is fed by decomposition of organic matter that is leached from soils (Wit et al., 2015). Model-based studies suggest Southeast Asia as a hotspot for river CO₂ emissions (Lauerwald et al., 2015; Raymond et al., 2013) due to the presence and degradation of carbon-rich peat soils.

About half of the known tropical peatlands are located in Southeast Asia, whereby 84% of these are Indonesian peatlands, mainly on the islands of Sumatra, Borneo and Irian Jaya (Page et al., 2011). Already in 2010, land use changes affected 90% of the peatlands located on Sumatra and Borneo (Miettinen and Liew, 2010) and turned them from CO₂ sinks to CO₂ sources (Hooijer et al., 2010). Enhanced decomposition in disturbed peatlands additionally increases the leaching of organic matter from soils into peat-draining rivers (Rixen et al., 2016; Moore et al., 2013). According to Regnier et al. (2013), land use



changes remobilize about (1.0 ± 0.5) Pg of soil organic carbon per year of which 40% are decomposed in rivers and emitted as
25 CO₂ to the atmosphere. The resulting CO₂ emissions of 0.4 PgC yr^{-1} represent 33% of the total CO₂ emissions from rivers
(Regnier et al., 2013).

Since peat soils are rich in carbon, concentrations of dissolved organic carbon (DOC) in peat-draining rivers are high and
increase with increasing peat coverage of the river catchments (Wit et al., 2015). However, despite high leaching rates and
DOC concentrations, measurement-based field studies find that CO₂ fluxes from rivers in Southeast Asia ($25.2 \text{ gC m}^{-2} \text{ yr}^{-1}$)
30 hardly exceed those in temperate zones ($18.5 \text{ gC m}^{-2} \text{ yr}^{-1}$, Wit et al., 2015; Müller et al., 2015). Possible reasons that were
suggested for these moderate emissions are short residence times of peat derived DOC in rivers due to the location of peatlands
near the coast (Müller et al., 2015) as well as the recalcitrant nature of DOC (Müller et al., 2016) and the lack of oxygen (O₂,
Wit et al., 2015) which both lower the rate of DOC decomposition. Borges et al. (2015) previously suggested a limitation of
bacterial production and the resulting DOC decomposition in African peat-draining rivers as consequence of low *pH* based on
35 observations at rivers in the Congo basin.

The assumption of low O₂ concentrations and *pH* as cause for moderate CO₂ emissions is supported by the regulating effect
of these parameters on decomposition rates in peat soils, where *pH* and O₂ are the key parameters that limit the activity of
the decomposition impelling enzyme phenol oxidase (Pind et al., 1994; Freeman et al., 2001). Studies agree that the limiting
effect of oxygen on decomposition rates is accurately represented by the Michaelis-Menten kinetics (Fang and Moncrieff,
40 1999; Pereira et al., 2017). This approach assumes that decomposition rates are linearly limited for low O₂ concentrations but
that there is no limitation for higher O₂ concentrations once they are sufficient to meet the decomposition demands (Keiluweit
et al., 2016). While peat-draining rivers are usually undersaturated with regard to atmospheric O₂ (Wit et al., 2015), their O₂
concentrations exceed those in peat soils due to gas exchange with the atmosphere (Müller et al., 2015; Rixen et al., 2008) and
thus are assumed to limit decomposition rates less strongly than in peat soils (Pind et al., 1994). The same applies for the *pH*
45 limitation, as *pH* in peat-draining rivers is usually higher than in peat soils (Pind et al., 1994). Other than for O₂ limitation,
however, the form of the *pH* limitation is still subject to discussion. Linear (Sinsabaugh, 2010) as well as exponential (Williams
et al., 2000; Kang et al., 2018) correlations have been stated in literature.

This study aims at quantifying the impact of *pH* and O₂ on the DOC decomposition in peat-draining rivers and the resulting
CO₂ emissions to the atmosphere. We analysed data from ten Southeast Asian peat-draining rivers with DOC concentrations
50 between $200 \mu\text{mol L}^{-1}$ and $3,000 \mu\text{mol L}^{-1}$ and *pH* and O₂ concentrations ranging from 3.8 to 7.1 and from $50 \mu\text{mol L}^{-1}$ to
 $200 \mu\text{mol L}^{-1}$, respectively.

2 Materials and methods

2.1 Study area

Southeast Asian peatlands store 42 Pg soil carbon across an area of 271,000 km² (Hooijer et al., 2010). More than 97% of
55 these peat soils are located in lowlands (Hooijer et al., 2006). The development of peatlands in Southeast Asia is favoured by



its tropical climate with high precipitation rates that range between 120 mm in July and 310 mm in November with an annual mean of 2,700 mm yr⁻¹ (Yatagai et al., 2020). Due to deforestation and conversion into plantations, today less than one-third of those Southeast Asian peatlands remain covered by peat swamp forests, while in 1990 it were more than three-quarters (Miettinen et al., 2016). Southeast Asian rivers mostly originate in mountain regions and cut through coastal peatlands on their way to the ocean (Fig. 1). Measurement data included in this study were obtained in river parts that flow through peat soils to capture the influence of peatlands on the carbon dynamics in the rivers.

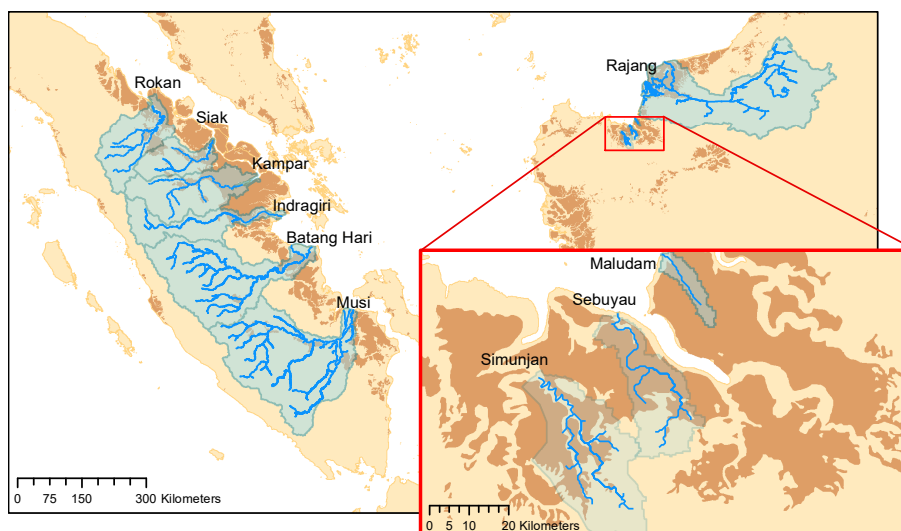


Figure 1. Map of river catchments with the location of peat areas. Blue lines indicate the main rivers. Blue shaded areas outline the river basins and brown areas indicate peatlands.

The collective data were derived from four rivers on Borneo (Sarawak, Malaysia) and six rivers on Sumatra (Indonesia). The investigated rivers on Borneo are the Rajang, Simunjan, Sebuyau and Maludam and the rivers surveyed on Sumatra are the Rokan, Kampar, Indragiri, Batang Hari, Musi and Siak (Fig. 1). We additionally include data from the Siak's tributaries Tapung Kiri, Tapung Kanan and Mandau. River peat coverages range from 4% in the Musi catchment to 91% in the Maludam catchment, whereby the bigger rivers that originate in the uplands generally have lower peat coverages than smaller coastal rivers.

2.2 Campaigns and measurements

Data were derived from a total of 16 campaigns in Sumatra and Sarawak (Tab. A1). For the Indonesian rivers, ten measurement campaigns between 2004 and 2013 were conducted. We use published data from Baum et al. (2007) for the Mandau, Tapung Kanan and Tapung Kiri rivers, from Wit et al. (2015) for the Siak, Indragiri, Batang Hari and Musi rivers and from Rixen et al. (2016) for the Rokan and Kampar rivers. CO₂ measurements are available for the campaigns performed after 2008.



For the Malaysian rivers, measurements were performed in six campaigns between 2014 and 2017. We use data published by Müller-Dum et al. (2018) for the Rajang river and by Müller et al. (2015) for the Maludam campaigns in 2014 and 2015. Additional campaigns for this study were conducted in March 2015 at the Simunjan and Sebuyau rivers as well as in January 2016, March 2017 and July 2017 at the Simunjan, Sebuyau and Maludam rivers. Measurements of DOC, CO₂ and O₂ concentrations as well as pH, water temperatures (*T*) and gas exchange coefficients (*k*₆₀₀) for these additional campaigns were performed in the same manner as during the 2014 Maludam campaign (Müller et al., 2015). However, due to technical problems, the CO₂, O₂ and pH data measured at the Simunjan river in 2016 were ignored for our analysis. Table 1 lists the averaged river parameters, including the catchments' peat coverages and atmospheric CO₂ fluxes.

Table 1. Measured data from the investigated rivers.

River	peat coverage (%)	pH	<i>T</i> (°C)	DOC (μmol L ⁻¹)	O ₂ (μmol L ⁻¹)	CO ₂ (μmol L ⁻¹)	<i>k</i> ₆₀₀ (cm h ⁻¹)	<i>F</i> _{CO₂} (gC m ⁻² d ⁻¹)
Musi	4.0 ± 0.1	6.9 ± 0.3	30.6 ± 0.3	244 ± 5	149 ± 43	128 ± 18	17 ± 4	2.8 ± 2.9
Batang Hari	5.4 ± 0.1	7.1 ± 0.3	30.0 ± 0.1	321 ± 4	163 ± 1	72 ± 1	17 ± 4	1.4 ± 0.4
Indragiri	11.4 ± 0.2	6.3 ± 0.3	31.5 ± 0.1	692 ± 5	89 ± 3	171 ± 4	17 ± 4	3.8 ± 1.2
Siak	25.9 ± 0.4	5.1 ± 0.5	30.0 ± 0.2	1,829 ± 601	53 ± 22	256 ± 21	17 ± 4	5.9 ± 2.6
Kampar	27.8 ± 0.5	6.4 ± 0.4	29.4 ± 0.7	1,280 ± 44	98 ± 43	n.d.	n.d.	n.d.
Rokan	18.6 ± 0.3	6.5 ± 0.1	28.9 ± 1.1	781 ± 53	114 ± 22	n.d.	n.d.	n.d.
Mandau	48.1 ± 0.8	4.8 ± 0.7	30.3 ± 2.3	2,484 ± 669	63 ± 25	n.d.	n.d.	n.d.
Tapung Kanan	53.4 ± 0.9	5.8 ± 0.7	30.3 ± 1.0	1,526 ± 169	86 ± 27	n.d.	n.d.	n.d.
Tapung Kiri	3.9 ± 0.1	6.3 ± 0.5	30.8 ± 2.2	640 ± 162	132 ± 50	n.d.	n.d.	n.d.
Rajang	7.7 ± 0.1	6.7 ± 0.1	28.8 ± 1.2	169 ± 32	190 ± 26	92 ± 16	9 ± 1	1.9 ± 1.8
Maludam	90.7 ± 1.5	3.8 ± 0.2	26.0 ± 0.5	4,031 ± 805	55 ± 36	281 ± 30	5 ± 2	6.5 ± 3.2
Sebuyau	60.7 ± 1.0	4.2 ± 0.2	27.8 ± 0.6	3,026 ± 1,047	61 ± 26	279 ± 34	9 ± 5	6.4 ± 4.9
Simunjan ₁	42.9 ± 0.7	5.3 ± 0.4	28.2 ± 0.6	1,533 ± 559	107 ± 21	248 ± 54	11 ± 5	5.7 ± 4.9
Simunjan ₂	42.9 ± 0.7	5.0 ± 0.3**	27.9 ± 0.3	8,366 ± 1,694	52 ± 19**	475 ± 67**	11 ± 5	11.2 ± 6.5**

Values are means of river campaigns. Data variability is given by the standard deviation of the measurements. *For the Simunjan, the March 2015 and July 2017 campaigns (Simunjan₁) were separated from the January 2016 and March 2017 campaigns (Simunjan₂) due to strong differences in the parameters. **Due to technical problems during the Simunjan campaign in January 2016, these values are only based on one measurement campaign.

During the January 2016, March 2017 and July 2017 campaigns, concentrations of particulate inorganic carbon (PIC) in form of CaCO₃ were measured. Discrete water samples, taken from approximately 1 m below the water surface, were filtered through pre-weighed and pre-combusted glass fiber filters (0.7 μm) to sample particulate material within the water volume. To determine the particulate carbon (organic and inorganic), the samples were then catalytically combusted at 1,050 °C and combustion products were measured by thermal conductivity using an Euro EA3000 Elemental Analyzer. The PIC was determined from the difference between this total particulate carbon and particulate organic carbon that was measured after addition of 1 molar hydrochloric acid in order to remove the inorganic carbon from the sample.



2.3 Additional parameters and catchment properties

Atmospheric CO₂ fluxes from the rivers were calculated from exchange coefficients and CO₂ concentrations according to

$$90 \quad F_{\text{CO}_2} = k_{\text{CO}_2}(T) \cdot (\text{CO}_2 - K_{\text{CO}_2}(T) \cdot p\text{CO}_2^{\text{a}}), \quad (1)$$

whereat $k_{\text{CO}_2}(T)$ was calculated from k_{600} according to Wanninkhof (1992). $p\text{CO}_2^{\text{a}}$ is the atmospheric partial pressure of CO₂ ($\approx 400 \mu\text{atm}$) and K_{CO_2} describes the temperature dependent Henry coefficient for CO₂, which was calculated according to Weiss (1974). The atmospheric O₂ fluxes (F_{O_2}) were derived analogously with $k_{\text{O}_2}(T)$ calculated according to Wanninkhof (1992) and Henry coefficients for O₂ calculated according to Weiss (1970).

95 Catchment sizes were derived from Hydro-SHEDS (Lehner et al., 2006) at 15 s resolution, using Esri's ArcMap 10.5. Sub-basins belonging to the catchments were identified using the HydroSHEDS 15 s flow directions data set and added to the main basins. Catchment areas were then determined using WGS 1984 Web Mercator Projection.

Peat maps were downloaded from www.globalforestwatch.org for Indonesia and Malaysia. The Indonesian peatland map was published by the Ministry of Agriculture in 2012. The Malaysian peat map was made available by Wetlands International in
100 2004 and is based on a national inventory by the Land and Survey Department of Sarawak (1968). Both maps include peatlands in different conditions, from undisturbed peat swamp forest to disturbed peat under plantations, which is nowadays widespread in those countries. Peat coverage was determined from the areal extent of peatlands in the catchment divided by catchment size. Peat coverages derived using other peat maps are compared in Appendix B.

2.4 Quantification of the pH and O₂ impact on decomposition rates

105 The decomposition rate of DOC (R) is defined as molecules of CO₂ that are produced per available molecules of DOC during a specific time step and thus represents the proportionality factor between the CO₂ production rate and the DOC concentration:

$$R = \frac{\Delta\text{CO}_2}{\text{DOC} \cdot \Delta t} \Rightarrow \frac{\partial\text{CO}_2}{\partial t} = R \cdot \text{DOC}. \quad (2)$$

As discussed before, R can be limited by O₂ concentrations and by pH. We used an O₂ limitation factor that is based on
110 the Michaelis-Menten equation ($L_{\text{O}_2} = \frac{\text{O}_2}{K_m + \text{O}_2}$) as suggested by Pereira et al. (2017). For pH limitation, we consider two approaches suggested in literature that are represented by an exponential limitation factor ($L_{\text{pH}} = \exp(\lambda \cdot (\text{pH} - \text{pH}_0))$) as suggested by Williams et al. (2000) and by a linear limitation factor ($L_{\text{pH}} = \frac{\text{pH}}{\text{pH}_0}$) as suggested by Sinsabaugh (2010).

For the exponential pH approach the CO₂ production rate due to DOC decomposition is given by

$$\frac{\partial\text{CO}_2}{\partial t} = R_{\text{max}} \cdot L_{\text{O}_2} \cdot L_{\text{pH}} \cdot \text{DOC} = R_{\text{max}} \cdot \frac{\text{O}_2}{K_m + \text{O}_2} \cdot \exp(\lambda \cdot (\text{pH} - \text{pH}_0)) \cdot \text{DOC}, \quad (3)$$

115 where R_{max} is the maximum decomposition rate, K_m is the Michaelis constant for O₂ inhibition that is also called the half saturation constant and gives the O₂ concentration at which O₂ limits decomposition by 50% (Loucks and Beek, 2017), λ is the pH inhibition constant and pH_0 is a normalization constant that was set to 7.5 since this is reported to be the optimal pH



for the activity of the decomposition impelling enzyme phenol oxidase (Pind et al., 1994; Kocabas et al., 2008). Equation (3) is only valid for $pH \leq pH_0$, as the limitation factor cannot be > 1 . For higher water pH , a different approach would be needed. However, for the rivers in this study Eq. (3) is sufficient since their pH is < 7.5 (Tab. 1). When O_2 concentrations and water pH are high enough not to limit the decomposition rate, Eq. (3) simplifies to Eq. (2) with $R = R_{max}$.

The dissolved inorganic carbon (DIC) concentrations in peat-draining rivers, as a first approximation, result from an equilibrium between CO_2 emissions and CO_2 production by decomposition. Therefore, we optimized the parameters in Eq. (3) such that the production of CO_2 in the water volume beneath a specific surface area equals the atmospheric CO_2 flux through this area. The CO_2 production is calculated by multiplication of Eq. (3) with the product of river depth d and surface area A and the CO_2 emissions are calculated by multiplication of Eq. (1) with the surface area A :

$$d \cdot A \cdot R_{max} \cdot \frac{O_2}{K_m + O_2} \cdot \exp(\lambda \cdot (pH - pH_0)) \cdot DOC = A \cdot k_{CO_2}(T) \cdot (CO_2 - K_{CO_2}(T) \cdot pCO_2^a). \quad (4)$$

Analogously, river O_2 concentrations result from an equilibrium between the atmospheric O_2 flux and O_2 consumption due to decomposition. During decomposition, the O_2 consumption is proportional to the CO_2 production ($\Delta O_2 = -b \cdot \Delta CO_2$). The proportionality factor b is usually < 1 since a fraction of the O_2 used for decomposition is taken from the oxygen content in the dissolved organic matter (Rixen et al., 2008). Thus, the equilibrium between O_2 consumption within the water volume and O_2 flux through the surface area can be written as

$$-b \cdot d \cdot A \cdot R_{max} \cdot \frac{O_2}{K_m + O_2} \cdot \exp(\lambda \cdot (pH - pH_0)) \cdot DOC = A \cdot k_{O_2}(T) \cdot (O_2 - K_{O_2}(T) \cdot pO_2^a). \quad (5)$$

In order to compare these dependencies to measured data, Eq. (4) and Eq. (5) were analytically solved for CO_2 and for O_2 , respectively. The resulting equations are listed in Tab. 2. The analogously derived equations for CO_2 and O_2 that result from the linear pH approach are listed in Tab. 3. Based on these equations, least squares optimizations were performed for the decomposition parameters R_{max} , b , K_m and λ such that $CO_2(DOC, pH, O_2)$ and $O_2(DOC, pH)$ are simultaneously optimized for the measured parameters of DOC , pH , T , CO_2 and O_2 .

Table 2. Equations to derive CO_2 and O_2 for the exponential pH approach.

$$CO_2(DOC, pH, O_2) = K_{CO_2}(T) \cdot pCO_2^a + \frac{d \cdot R_{max} \cdot DOC \cdot \frac{O_2}{K_m + O_2} \cdot \exp(\lambda \cdot (pH - pH_0))}{k_{CO_2}(T)}$$

$$O_2(DOC, pH) = \sqrt{\left(\frac{b \cdot d \cdot R_{max} \cdot DOC \cdot \exp(\lambda \cdot (pH - pH_0)) + k_{O_2}(T) \cdot (K_m - K_{O_2}(T) \cdot pO_2^a)}{2 \cdot k_{O_2}(T)} \right)^2 + K_{O_2}(T) \cdot pO_2^a \cdot K_m} - \frac{b \cdot d \cdot R_{max} \cdot DOC \cdot \exp(\lambda \cdot (pH - pH_0)) + k_{O_2}(T) \cdot (K_m - K_{O_2}(T) \cdot pO_2^a)}{2 \cdot k_{O_2}(T)}$$

Equations to derive CO_2 from measured DOC , pH and O_2 as well as to derive O_2 from measured DOC and pH . The parameters R_{max} , K_m , λ and b were derived by least squares optimization based on measured DOC , pH , T , O_2 and CO_2 data of the investigated rivers.

The equations in Tab. 2 and Tab. 3 depend on the river gas exchange coefficients for CO_2 (k_{CO_2}) and O_2 (k_{O_2}), which both depend on k_{600} . Those exchange coefficients are poorly constrained and spatial as well as temporal extremely variable. The k_{600} we list in this study are based on a variety of techniques, including floating chamber measurements, calculations based on wind speed and catchment parameters and balance models of water parameters. Although all of those estimates remain



highly uncertain, we find a fairly good agreement between k_{600} and river depths (d , Fig. A1). We therefore use a fixed ratio of $k_{600}/d = (7.0 \pm 0.5) \cdot 10^{-6} \text{ s}^{-1}$ for the least squares approximations.

Table 3. Equations to derive CO_2 and O_2 for the linear pH approach.

$$\text{CO}_2(\text{DOC}, \text{pH}, \text{O}_2) = K_{\text{CO}_2}(T) \cdot p\text{CO}_2^a + \frac{d \cdot R_{\text{max}} \cdot \text{DOC} \cdot \frac{\text{O}_2}{K_m + \text{O}_2} \cdot \frac{\text{pH}}{\text{pH}_0}}{k_{\text{CO}_2}(T)}$$

$$\text{O}_2(\text{DOC}, \text{pH}) = \sqrt{\left(\frac{b \cdot d \cdot R_{\text{max}} \cdot \text{DOC} \cdot \frac{\text{pH}}{\text{pH}_0} + k_{\text{O}_2}(T) \cdot (K_m - K_{\text{O}_2}(T) \cdot p\text{O}_2^a)}{2 \cdot k_{\text{O}_2}(T)} \right)^2 + K_{\text{O}_2}(T) \cdot p\text{O}_2^a \cdot K_m} - \frac{b \cdot d \cdot R_{\text{max}} \cdot \text{DOC} \cdot \frac{\text{pH}}{\text{pH}_0} + k_{\text{O}_2}(T) \cdot (K_m - K_{\text{O}_2}(T) \cdot p\text{O}_2^a)}{2 \cdot k_{\text{O}_2}(T)}}$$

Equations to derive CO_2 from measured DOC, pH and O_2 as well as to derive O_2 from measured DOC and pH . The parameters R_{max} , K_m , λ and b were derived by least squares optimization based on measured DOC, pH , T , O_2 and CO_2 data of the investigated rivers.

145 3 Results

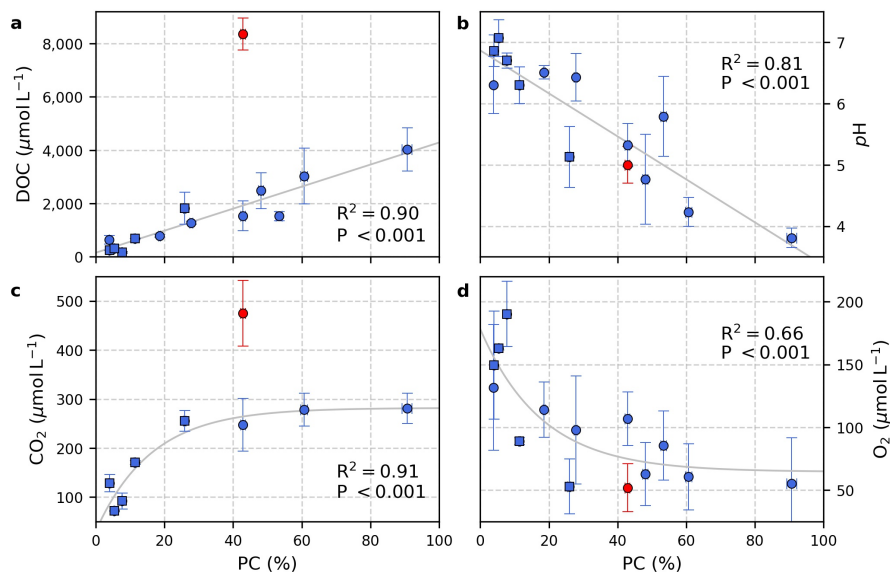


Figure 2. Correlation of peat coverage (PC) with (a) DOC, (b) pH , (c) CO_2 & (d) O_2 . Each data point represents one river. Variability is indicated by the error bars, which are given by standard deviation. For the Simunjan river, the January 2016 and March 2017 campaigns (Simunjan₂, see Tab. 1 and Tab. 4), indicated by red data points, were separated from the other Simunjan campaigns (Simunjan₁) and excluded from the correlations due to strong deviations from the other campaigns that imply an additional process discussed in Sect. 4.3. Ordinary least squares approximations were used to calculate linear correlations with DOC and pH and exponential correlations with CO_2 and O_2 . Rivers included in a previous study investigating these correlations (Wit et al., 2015) are indicated by squares.



3.1 Correlation with peat coverage

The data presented in Tab. 1 yield a linear increase of river DOC concentration with peat coverage (Fig. 2a) as well as a negative linear correlation between river pH and peat coverage (Fig. 2b). The river CO_2 concentration shows a strong increase for peat coverages $< 30\%$. Yet, despite further increase in DOC concentrations, CO_2 concentrations in rivers with peat coverage $> 30\%$ level off, resulting in a fairly constant CO_2 for peat coverages $> 50\%$ (Fig. 2c). The river O_2 shows an opposite behaviour to the CO_2 . O_2 concentrations initially decrease with increasing peat coverage and show a decline in the regression rate for high peat coverages, resulting in a minimum O_2 concentration of approximately $65 \mu\text{mol L}^{-1}$ (Fig. 2d).

However, the Simunjan seems to be an exception. Although we found that generally CO_2 concentrations stagnate for high peat coverages, extremely high CO_2 concentrations were measured during two campaigns in the Simunjan river (Fig. 2). In January 2016 and March 2017 (Simunjan₂) DOC and CO_2 concentrations in the Simunjan river were significantly higher than in March 2015 and July 2017 (Simunjan₁, Tab. 4). O_2 concentrations during these campaigns were lower ($\approx 50 \mu\text{mol L}^{-1}$) than for the other Simunjan campaigns ($\approx 107 \mu\text{mol L}^{-1}$), while the water pH of 5.0 was only slightly lower than during the other campaigns ($pH \approx 5.3$). The Simunjan campaigns with high DOC and CO_2 concentrations were accompanied by high concentrations of particulate carbonate ($CaCO_3$, Tab. 4), while $CaCO_3$ concentrations in July 2017 were much lower.

Table 4. Data measured in the four Simunjan campaigns.

	Campaign	pH	DOC (mmol L^{-1})	CO_2 ($\mu\text{mol L}^{-1}$)	O_2 ($\mu\text{mol L}^{-1}$)	$CaCO_3$ (mg L^{-1})
Simunjan ₁	Mar 2015	5.2 ± 0.3	1.7 ± 0.7	268 ± 71	99 ± 10	n.d.
Simunjan ₂	Jan 2016	$4.5 \pm 0.3^*$	9.4 ± 1.2	$> 330^{**}$	$139 \pm 9^*$	0.52 ± 0.34
Simunjan ₂	Mar 2017	5.0 ± 0.3	7.4 ± 0.6	475 ± 97	52 ± 19	0.63 ± 0.64
Simunjan ₁	Jul 2017	5.4 ± 0.3	1.4 ± 0.3	227 ± 16	115 ± 14	0.07 ± 0.05

Values are means of measurements. Data variability is given by standard deviation of measurements. *Due to technical problems, the March 2017 pH , CO_2 and O_2 data need to be treated cautiously. **In March 2017 only a minimum CO_2 concentration could be derived.

3.2 Limitation of decomposition rates by pH and O_2

In order to gain a better understanding of the pH and O_2 impacts on decomposition rates, we examined correlations of CO_2 and O_2 concentrations that were calculated based on the dependencies derived from both the linear (Tab. 3) and exponential (Tab. 2) approach of pH limitation with measured data. Figure 4 shows the correlation for linear pH limitation. Coefficients of determination for the CO_2 and O_2 correlations result to $R^2 = 0.80$ and $R^2 = 0.87$, respectively.

The decomposition parameters for this linear pH approach, derived via least squares approximation of the equation in Tab. 3 to measured data, result to a Michaelis constant for O_2 limitation of $K_m = (390 \pm 509) \mu\text{mol L}^{-1}$, a maximum decomposition rate of $R_{\text{max}} = (10 \pm 11) \mu\text{mol mol}^{-1} \text{s}^{-1}$ and a fraction of O_2 consumption of $b = (90 \pm 25)\%$. These values represent pH limitations in the rivers that lower decomposition rates and therewith CO_2 production by between 6% in the Batang Hari and



49% in the Maludam, while the O₂ limitations lower decomposition rates by between 71% in the Batang Hari and 88% in the
170 Maludam and the Siak.

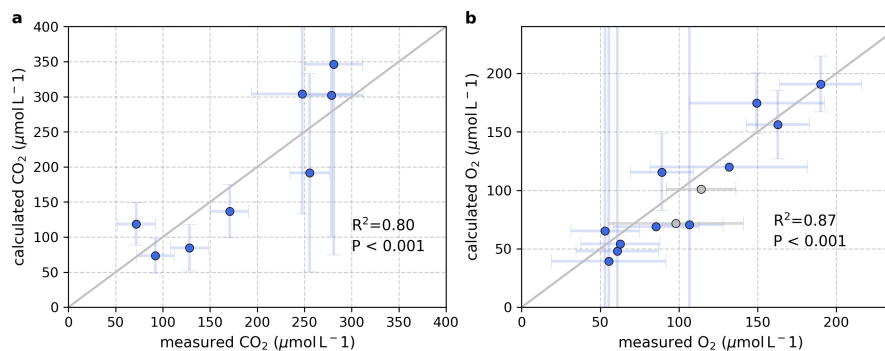


Figure 3. Correlation between measured and calculated concentrations of (a) CO₂ and (b) O₂. Calculations were based on the equations in Tab. 3 which represent linear *pH* limitation of decomposition rates. Each data point represents one river. Grey data points are excluded from the correlation since the data for these rivers (Kampar and Rokan) are based on less than three campaigns within the same season.

Figure 4 shows the CO₂ and O₂ correlations for exponential *pH* limitation of decomposition. The resulting correlation for CO₂ ($R^2 = 0.89$) is stronger than for the linear approach, while the O₂ correlation, with $R = 0.85$, is slightly weaker. The decomposition parameters that were derived for the exponential *pH* limitation are listed in Tab. 5.

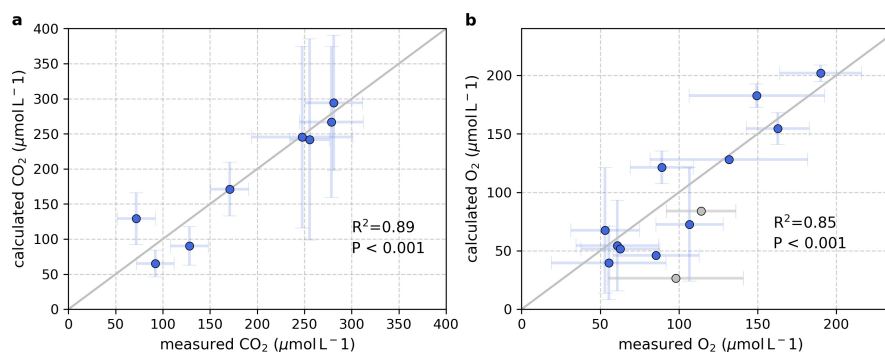


Figure 4. Correlation between measured and calculated concentrations of (a) CO₂ and (b) O₂. Calculations were based on the equations in Tab. 2 which represent exponential *pH* limitation of decomposition rates. Each data point represents one river. Grey data points are excluded from the correlation since the data for these rivers (Kampar and Rokan) are based on less than three campaigns within the same season.

The Michaelis constant for O₂ derived for the exponential limitation, with $K_m \approx 6 \mu\text{mol L}^{-1}$ is significantly smaller than the
175 constant derived for linear *pH* limitation. The maximum decomposition rate ($R_{\text{max}} \approx 4 \mu\text{mol mol}^{-1} \text{s}^{-1}$) and the fraction of O₂ consumption ($b \approx 81\%$), while being in the same order of magnitude, are also smaller than for linear *pH* limitation. The exponential *pH* limitation factor results to $\lambda \approx 0.5$. O₂ limitation, resulting from these parameters, limits decomposition in the



investigated rivers by $\leq 10\%$, while pH limitation ranges between 20% in the Batang Hari and 85% in the Maludam. The total limitation by O_2 and pH ranges between 23 and 87% (Tab. 6).

Table 5. Decomposition parameters optimized via least squares approximation for the exponential pH approach.

parameter	value	unit
R_{\max}	4.0 ± 0.8	$\mu\text{molCO}_2 \text{ mol}^{-1}\text{DOC s}^{-1}$
b	81 ± 10	%
K_m	6 ± 26	$\mu\text{mol L}^{-1}$
λ	0.52 ± 0.10	

Data were derived for exponential pH limitation of decomposition via least squares optimization of the equations in Tab. 2.

Table 6. pH and O_2 limitations calculated for individual rivers.

River	pH lim. (%)	O_2 lim. (%)	total lim. (%)	River	pH lim. (%)	O_2 lim. (%)	total lim. (%)
Musi	28 ± 5	4 ± 1	31 ± 5	Tapung Kanan	59 ± 7	7 ± 2	62 ± 7
Batang Hari	20 ± 3	4 ± 1	23 ± 4	Tapung Kiri	46 ± 6	4 ± 1	49 ± 7
Indragiri	46 ± 6	6 ± 2	50 ± 7	Rajang	34 ± 5	3 ± 1	36 ± 5
Siak	71 ± 7	10 ± 5	74 ± 8	Maludam	85 ± 5	10 ± 4	87 ± 6
Kampar	43 ± 6	6 ± 1	46 ± 7	Sebuyau	83 ± 6	9 ± 4	83 ± 6
Rokan	40 ± 6	5 ± 1	43 ± 6	Simunjan	68 ± 7	5 ± 1	70 ± 7
Mandau	76 ± 7	9 ± 3	78 ± 7				

Fraction by which the decomposition is lowered due to the impact of pH and O_2 , calculated based on the limitation factors in Eq. (3) and the parameters in Tab. 5 according to pH lim. = $(1 - L_{pH})$, O_2 lim. = $(1 - L_{O_2})$ and total lim. = $(1 - L_{pH} \cdot L_{O_2})$.

180 4 Discussion

4.1 Carbon dynamics in peat-draining rivers

The linear correlations observed between peat coverage and DOC (Fig. 2a) as well as pH (Fig. 2b) agree with results by Wit et al. (2015) and confirm the importance of peat soils as a major DOC source to these rivers, whereas the decomposition of DOC and leaching of organic acids from peat areas lower the pH . The initial increase of CO_2 concentrations (Fig. 2c) and decrease of O_2 concentrations (Fig. 2d) with peat coverage can be explained by increased DOC decomposition due to higher DOC concentrations and also agrees with the results of Wit et al. (2015).

The CO_2 stagnation we observe for rivers of higher peat coverages (Fig. 2c) agrees with moderate CO_2 emissions that were stated for those rivers (Müller et al., 2015; Moore et al., 2013) and according to Eq. (3) can be explained by the pH limitation.



190 A similar pattern of stagnating CO₂ concentrations has been observed in river sections of high DOC at the Congo river (Borges et al., 2015), indicating that the underlying process is valid not only for Southeast Asian rivers but for tropical peat-draining rivers in general.

4.2 Exponential pH limitation of decomposition rates

195 As shown, we were able to reproduce the stagnation in CO₂ and O₂ concentrations by introducing O₂ and pH limitations for decomposition rates in the rivers. Model approaches of both exponential and linear pH limitation reproduce the observed stagnation in CO₂ and O₂ concentrations and result in reasonably good correlations with the measured concentrations (Fig. 4 and Fig. 3).

The fractions of O₂ consumption by decomposition that we derived for both approaches, with $b = (81 \pm 10)\%$ and $b = (90 \pm 25)\%$, agree with the fraction of 0.8 that was calculated based on the oxygen to carbon ratio in peat soils (Rixen et al., 2008). The maximum decomposition rates of $4 \mu\text{mol mol}^{-1} \text{s}^{-1}$ for the exponential approach and $10 \mu\text{mol mol}^{-1} \text{s}^{-1}$ for the linear 200 approach agree with global soil phenol oxidase activity data published by Sinsabaugh et al. (2008) that stated global average soil phenol oxidase activity of $70.6 \mu\text{mol h}^{-1}$ per g organic matter. For a carbon content in organic matter of 38 mmol g^{-1} (Sinsabaugh, 2010) this represents approximately $0.5 \mu\text{mol mol}^{-1} \text{s}^{-1}$, while sites of high phenol oxidase activity are listed with up to $3 \mu\text{mol mol}^{-1} \text{s}^{-1}$ (Sinsabaugh et al., 2008).

205 However, we assume the exponential limitation to be more realistic than the linear limitation as it is better in representing river CO₂ especially for high CO₂ concentrations which are most strongly effected by the pH limitation. This assumption is supported by the unrealistically high O₂ limitation resulting from the linear approach, which yields a Michaelis constant of $K_m \approx 390 \mu\text{mol L}^{-1}$. Since the Michaelis constant represents the O₂ concentration at which decomposition is limited by 50% a Michaelis constant that, as in this case, is higher than the O₂ concentration in atmospheric equilibrium ($\approx 280 \mu\text{mol L}^{-1}$) would imply an oxygen deficit at atmospheric conditions that does not exist (Vaquer-Sunyer and Duarte, 2008). In literature, 210 Michaelis constants between 1 and $40 \mu\text{mol L}^{-1}$ are suggested for the O₂ impact on phenol oxidase, depending on the phenolic species (Fenoll et al., 2002).

The Michaelis constant for O₂ derived with exponential pH limitation ($K_m \approx 6 \mu\text{mol L}^{-1}$) is in good agreement with the literature data of 1 to $40 \mu\text{mol L}^{-1}$ (Fenoll et al., 2002). Its large uncertainty ($> 400\%$, Tab. 5) is caused by relatively high concentrations of O₂ in the rivers. Due to exchange with atmospheric O₂ the concentrations in all rivers exceed the median 215 O₂ threshold to lethal hypoxic conditions of $50 \mu\text{mol L}^{-1}$ (Vaquer-Sunyer and Duarte, 2008). Thus, the O₂ limitation in peat-draining rivers is relatively small (between 3 and 10%, Tab. 6) and consequentially a majority of the limitation is caused by the low pH in peat-draining rivers that we found to limit the decomposition rates in rivers of high peat coverage (low pH) by up to 85% (Tab. 6).

220 The calculated exponential pH coefficient of $\lambda = 0.5 \pm 0.1$ is similar to coefficients reported for high latitude peat soils ($\lambda = 0.65$ & $\lambda = 0.77$) that were determined via laboratory measurements of phenol oxidase activity (Williams et al., 2000). The



fact that the exponential inhibition by pH can be found in those high latitude peat soils as well as in tropical peat-draining rivers suggests that the investigated correlations and processes are also relevant in other regions and that soil and water pH are important regulators of global carbon emissions.

4.3 Disruption of the pH limitation by carbonates

225 Typically, concentrations of particulate carbonate in peat-draining rivers are low (Wit et al., 2018). However we observed high $CaCO_3$ concentrations for the Simunjan₂ campaigns, which show high DOC and CO_2 concentrations (Tab. 4). Possible causes for high carbonate concentrations during these campaigns could be increased erosion of mineral soils due to deforestation in mountain regions upstream or liming practices in plantations along the river. In either case, high carbonate concentrations at such a low pH indicate high dissolution of carbonates which might have counteracted a decrease in pH due to decomposition
230 of DOC. This seems to have suspended the natural pH limitation of decomposition in peat-draining rivers which could explain the high CO_2 concentrations observed during those two Simunjan campaigns (Tab. 4).

4.4 Implications and outlook

The stagnation in CO_2 we observe for high peat coverages provides an explanation for the disagreement between model studies that state extremely high CO_2 emissions from Southeast Asian rivers (Raymond et al., 2013; Lauerwald et al., 2015) and
235 measurement-based studies that state rather moderate emission rates (Wit et al., 2015; Müller et al., 2015). The pH limitation of decomposition that we derive to explain the observed CO_2 stagnation should be included to improve future model studies and accurately capture river CO_2 emissions from tropical peat areas.

The response on carbonate enrichment that we observe at the Simunjan river represents another important process that should be considered for anthropogenic activities like liming and enhanced weathering. Liming is a common practice to enhance soil
240 fertility in plantations and enhanced weathering is a carbon dioxide removal strategy (Field and Mach, 2017) during which atmospheric CO_2 is transformed into carbonates (Beerling et al., 2020). The resultant increase in carbonate concentrations and pH could cause a strong increase of decomposition rates and thereby CO_2 production and emission that would counteract the CO_2 uptake, which is not included in current estimates of enhanced weathering efficiencies (Taylor et al., 2016; Beerling et al., 2020).

245 5 Conclusions

Our study shows that CO_2 concentrations in and emissions from Southeast Asian rivers stagnate for high peat coverages of the river catchments. Despite further increases in river DOC concentrations, CO_2 concentrations are fairly constant for peat coverages $> 50\%$. We found that this stagnation is caused by low water pH in rivers of high peat coverage that hampers decomposition rates. This process provides an answer to the question why, in contrast to the high DOC export, CO_2 emissions
250 from tropical peat-draining rivers are more moderate.



We found an exponential limitation of decomposition by pH . Our calculations suggest that the low pH in rivers of high peat coverage reduces decomposition rates and thereby CO_2 production within the rivers by up to 85%. Although this study is based on measurements in Southeast Asian peat-draining rivers, comparisons to laboratory studies of decomposition in temperate peat soils suggest that the investigated correlations and processes are also relevant in other regions and that soil and water pH are important regulators of global carbon emissions.

As observed in the Simunjan river, one cause for increased water pH in peat-draining rivers can be the input of carbonates. We found that CO_2 concentrations during the Simunjan campaigns that were accompanied by enhanced concentrations of suspended carbonates were significantly higher than those during campaigns of low carbonate concentrations, resulting in CO_2 emissions from this river that were increased by almost 100%. We discussed that sources for enhanced carbonate concentrations can be rock weathering or soil erosion upstream of coastal peatland areas, or liming practices in plantations along the rivers, which are common practice to improve plant growth on acidic soils.

This carbonate impact should be considered when discussing the efficiency of enhanced weathering, which is discussed as one of the possible measures to extract and bind anthropogenic CO_2 by transferring it to carbonate. The resultant pH increase, in regions of high peat coverage could lead to enhanced decomposition and thereby emissions of CO_2 from rivers and soils. Further studies are needed to quantify the impact of the derived processes on enhanced weathering efficiencies.

Author contributions. AK performed the analysis and led the writing of the paper jointly with TR and TW. DM provided calculations of catchment parameters and in-depth comments on the manuscript. MM coordinated the field data collection in Malaysia. JN contributed to the data interpretation. All authors discussed results and commented on the manuscript.

Competing interests. The authors declare that they have no conflict of interest

Acknowledgements. We are grateful to the Sarawak Forestry Department and Sarawak Biodiversity Centre for permission to conduct collaborative research in Sarawak under permit numbers NPW.907.4.4(Jld.14)-161, SBC-RA-0097-MM, and Park Permit WL83/2017.



Appendix A: Additional Figures & Tables

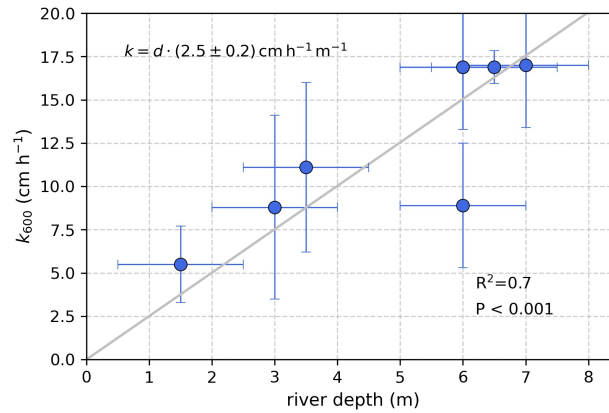


Figure A1. Correlation between atmospheric exchange coefficients (k_{600}) and river depth. A linear correlation reveals a slope of $k_{600}/d = (2.5 \pm 0.2) \text{ cm h}^{-1} \text{ m}^{-1} = (7.0 \pm 0.5) \cdot 10^{-6} \text{ s}^{-1}$.



Table A1. List of river campaigns

River	03.04	09.04	08.05	03.06	04.06	11.06	03.08	10.09	10.12	04.13	03.14	03.15	01.16	08.16	03.17	07.17
Maludam	-	-	-	-	-	-	-	-	-	-	✓	✓	✓	-	✓	✓
Sebuyau	-	-	-	-	-	-	-	-	-	-	-	✓	✓	-	✓	✓
Simunjan	-	-	-	-	-	-	-	-	-	-	-	✓	✓	-	✓	✓
Rajang	-	-	-	-	-	-	-	-	-	-	-	-	✓	✓	✓	-
Musi	-	-	-	-	-	-	-	✓	✓	✓	-	-	-	-	-	-
Batang Hari	-	-	-	-	-	-	-	✓	✓	✓	-	-	-	-	-	-
Indragiri	-	-	-	-	-	-	-	✓	-	✓	-	-	-	-	-	-
Kampar	-	-	-	-	✓	-	✓	-	-	-	-	-	-	-	-	-
Rokan	-	-	-	-	✓	-	✓	-	-	-	-	-	-	-	-	-
Siak	✓	✓	✓	✓	-	✓	-	✓	-	✓	-	-	-	-	-	-
Mandau	✓	✓	✓	✓	-	-	-	-	-	-	-	-	-	-	-	-
Tapung Kanan	✓	✓	✓	✓	-	-	-	-	-	-	-	-	-	-	-	-
Tapung Kiri	✓	✓	✓	✓	-	-	-	-	-	-	-	-	-	-	-	-



Appendix B: Comparison of different peat coverage estimates

275 Different peat maps are available for Southeast Asia and the approaches to determine peat coverage of river catchments were inconsistent among different studies cited in our paper. We want to show here that the choice of a data product is crucial for the determination of peat coverage. We are comparing three different products (Tab. B1): The FAO Digital Soil Map of the World, Country products downloaded at Global Forest Watch and the Center for International Forestry Research (CIFOR) Wetlands distribution.

Table B1. Different data products used to assess peatland extent in the catchments.

FAO	
Product	Food and Agriculture Organization of the United Nations (FAO): Digital Soil Map of the World
Coordinate System	WGS 1984
Reference	FAO Land and Water Development Division. Digital Soil Map of the World. Version 3.6. Rome, Italy 2003.
Website	http://www.fao.org/geonetwork/srv/en/metadata.show?id=14116
Notes	Peatlands were identified as Histosols. On Sumatra and Borneo, these are Dystric Histosols (“Od”)
GFW	
Product	Global Forest Watch Country products
Coordinate System	WGS 1984
Reference	Indonesia: Ministry of Agriculture. Indonesia peat lands, 2012. Malaysia: Wetlands International. "Malaysia peat lands", 2004.
Website	www.globalforestwatch.org
CIFOR	
Product	Center for International Forestry Research (CIFOR): Tropical and Subtropical Wetlands Distribution version 2.
Coordinate System	WGS 1984
Reference	Data product: Gumbricht et al. (2018); Related publication: Gumbricht et al. (2017)
Website	https://data.cifor.org/dataset.xhtml?persistentId=doi:10.17528/CIFOR/DATA.00058
Notes	Of the three available files, the product used was TROP_SUBTROP_PeatV21_2016_CIFOR.7z

280 Those three products lead to highly different results (Tab. B2). We observed a tendency that CIFOR leads to smaller peat coverage than FAO and GFW. This is because CIFOR misses some, but not all peat areas that are known to be under industrial plantations. Gumbricht et al. (2017) already pointed out that their model underestimates peatland area in Sumatra because peats are largely drained, which the model does not capture. However, in the Musi and Batang Hari catchment, CIFOR sees larger peat areas than FAO and GFW, which means that some peatlands might be missing in those maps.



Table B2. Results for peat coverage (PC) in the different catchments using the three different data products.

River name	Catchment (km ²)	PC GFW	PC CIFOR	PC FAO
Batang Hari	43,778	5.4 ± 0.1	6.8 ± 0.1	5.0 ± 0.1
Indragiri	17,713	11.4 ± 0.2	9.6 ± 0.1	8.6 ± 0.1
Kampar	23,610	27.8 ± 0.4	20.2 ± 0.2	18.8 ± 0.3
Musi	57,602	4.0 ± 0.1	11.3 ± 0.1	3.7 ± 0.1
Rokan	19,953	18.4 ± 0.3	8.8 ± 0.1	30.3 ± 0.5
Siak	11,719	25.9 ± 0.4	14.8 ± 0.1	27.2 ± 0.4
Maludam	91	90.7 ± 1.4	82.3 ± 1.1	100.0 ± 1.5
Rajang	51,699	7.7 ± 0.1	7.4 ± 0.1	10.6 ± 0.2
Sebuyau	451	60.7 ± 0.9	41.2 ± 0.4	75.8 ± 1.2
Simunjan	755	42.9 ± 0.7	20.3 ± 0.2	25.9 ± 0.4

We decided to use the GFW maps for several reasons: 1) CIFOR seems to miss peat under industrial plantations, which is still relevant for river carbon dynamics. Therefore, we chose not to use the CIFOR maps. 2) Between GFW and FAO, GFW is more recent than FAO for Indonesia. For Sarawak (Malaysia), both are based on the 1968 soil map by the Land Survey Department, but FAO uses a 10-fold coarser scale than the 1968 soil map (1:5,000,000 compared to 1:500,000). Thus, the GFW product was used. & 3) GFW maps are based on official information, and we believe that the local authorities would know best about the peatland distribution in their country.

Similar to the peat coverage, the publications from which we use data in our study all had different approaches to determining catchment size – either including (Müller-Dum et al., 2018) or excluding (Wit et al., 2015) smaller sub-catchments. In our study, we aimed to unify those different approaches. Therefore, we recalculated catchment areas from one single data product (HydroSHEDS, (Lehner et al., 2006)) including sub-catchments that were identified using HydroSHEDS flow directions. The Simunjan catchment is included in the bigger Sadong catchment in HydroSHEDS. Therefore, it was manually delineated using HydroSHEDS flow directions.



References

- Aufdenkampe, A. K., Mayorga, E., Raymond, P. A., Melack, J. M., Doney, S. C., Alin, S. R., Aalto, R. E., and Yoo, K.: Riverine coupling of biogeochemical cycles between land, oceans and atmosphere, *Front Ecol Environ*, <https://doi.org/10.1890/100014>, 2011.
- Baum, A., Rixen, T., and Samiaji, J.: Relevance of peat draining rivers in central Sumatra for the riverine input of dissolved organic carbon into the ocean, *Estuarine, Coastal and Shelf Science*, *73*, 563–570, <https://doi.org/10.1016/j.ecss.2007.02.012>, 2007.
- Beerling, D. J., Kantzas, E. P., Lomas, M. R., Wade, P., Eufrasio, R. M., Renforth, P., Sarkar, B., Andrews, M. G., James, R. H., James, R. H., Pearce, C. R., Mercure, J.-F., Pollitt, H., Holden, P. B., Edwards, N. R., Khanna, M., Koh, L., Quegan, S., Pidgeon, N. F., Janssens, I. A., Hansen, J., and Banwart, S. A.: Potential for large-scale CO₂ removal via enhanced rock weathering with croplands, *Nature*, *583*, <https://doi.org/10.1038/s41586-020-2448-9>, 2020.
- Borges, A. V., Darchambeau, F., Teodoru, C. R., Marwick, T. R., Tamooch, F., Geeraert, N., Omengo, F. O., Guérin, F., Lambert, T., Morana, C., Okuku, E., and Bouillon, S.: Globally significant greenhouse-gas emissions from African inland waters, *Nature Geoscience*, <https://doi.org/10.1038/ngeo2486>, 2015.
- Cole, J. J., Prairie, Y. T., Caraco, N. F., McDowell, W. H., Tranvik, L. J., Striegl, R. G., Duarte, C. M., Kortelainen, P., Downing, J. A., Middelburg, J. J., and Melack, J.: Plumbing the global carbon cycle, *Ecosystems*, <https://doi.org/10.1007/s10021-006-9013-8>, 2007.
- Fang, C. and Moncrieff, J.: A model for soil CO₂ production and transport 1: Model development, *Agricultural and Forest Meteorology*, *95*, 225 – 236, [https://doi.org/https://doi.org/10.1016/S0168-1923\(99\)00036-2](https://doi.org/https://doi.org/10.1016/S0168-1923(99)00036-2), <http://www.sciencedirect.com/science/article/pii/S0168192399000362>, 1999.
- Fenoll, L. G., Rodríguez-López, J. N., Graciá-Molina, F., Graciá-Cánovas, F., and Tudela, J.: Michaelis constants of mushroom tyrosinase with respect to oxygen in the presence of monophenols and diphenols, *The International Journal of Biochemistry & Cell Biology*, *34*, 332 – 336, [https://doi.org/https://doi.org/10.1016/S1357-2725\(01\)00133-9](https://doi.org/https://doi.org/10.1016/S1357-2725(01)00133-9), 2002.
- Field, C. B. and Mach, K. J.: Rightsizing carbon dioxide removal, *Science*, *356*, 706–707, <https://doi.org/10.1126/science.aam9726>, 2017.
- Freeman, C., Ostle, N., and Kang, H.: An enzymic ‘latch’ on a global carbon store, *Nature*, *409*, 149, <https://doi.org/10.1038/35051650>, 2001.
- Gumbricht, T., Roman-Cuesta, R. M., Verchot, L., Herold, M., Wittmann, F., Householder, E., Herold, N., and Murdiyarso, D.: An expert system model for mapping tropical wetlands and peatlands reveals South America as the largest contributor, *Global Change Biology*, *23*, 3581–3599, <https://doi.org/10.1111/gcb.13689>, 2017.
- Gumbricht, T., Román-Cuesta, R., Verchot, L., Herold, M., Wittmann, F., Householder, E., Herold, N., and Murdiyarso, D.: Tropical and Subtropical Wetlands Distribution version 2, <https://doi.org/10.17528/CIFOR/DATA.00058>, 2018.
- Hooijer, A., Silvius, M., and H. Wösten, and, S. P.: PEAT-CO₂, Assessment of CO₂ emissions from drained peatlands in SE Asia, Delft Hydraulics report Q3943, 2006.
- Hooijer, A., Page, S., Canadell, J. G., Silvius, M., Kwadijk, J., Wösten, H., and Jauhiainen, J.: Current and future CO₂ emissions from drained peatlands in Southeast Asia, *Biogeosciences*, *7*, 1505–1514, <https://doi.org/10.5194/bg-7-1505-2010>, 2010.
- Kang, H., Kwon, M. J., Kim, S., Lee, SeunghoonRogelj, J., Jones, T. G., Johncock, A. C., Haraguchi, A., and Freeman, C.: Biologically driven DOC release from peatlands during recovery from acidification, *Nature Communications*, *9*, <https://doi.org/10.1038/s41467-018-06259-1>, 2018.
- Keiluweit, M., Nico, P. S., Kleber, M., and Fendorf, S.: Are oxygen limitations under recognized regulators of organic carbon turnover in upland soils?, *Biogeochemistry*, <https://doi.org/10.1007/s10533-015-0180-6>, 2016.



- Kocabas, D. S., Bakir, U., Phillips, S. E. V., McPherson, M. J., and Ogel, Z. B.: Purification, characterization, and identification of a novel bifunctional catalase-phenol oxidase from *Scytalidium thermophilum*, *Appl Microbiol Biotechnol*, 79, 407–415, <https://doi.org/10.1007/s00253-008-1437-y>, 2008.
- Lauerwald, R., Laruelle, G. G., Hartmann, J., Ciais, P., and Regnier, P. A. G.: Spatial patterns in CO₂ evasion from global river network, *Global Biogeochemical Cycles*, 29, 534–554, <https://doi.org/10.1002/2014GB004941>, 2015.
- Lehner, B., Verdin, K., and Jarvis, A.: HydroSHEDS, Technical Documentation, Tech. rep., HydroSHEDS, version 1.0, Pages 1–27, 2006.
- Loucks, P. and Beek, E.: Water Quality Modeling and Prediction, pp. 417–467, https://doi.org/10.1007/978-3-319-44234-1_10, 2017.
- Miettinen, J. and Liew, S. C.: Degradation and development of peatlands in Peninsular Malaysia and in the islands of Sumatra and Borneo since 1990, *Land Degradation & Development*, 21, 285–296, <https://doi.org/10.1002/ldr.976>, 2010.
- Miettinen, J., Shi, C., and Liew, S. C.: Land cover distribution in the peatlands of Peninsular Malaysia, Sumatra and Borneo in 2015 with changes since 1990, *Global Ecology and Conservation*, 6, 67–78, <https://doi.org/10.1016/j.gecco.2016.02.004>, 2016.
- Moore, S., Evans, C. D., Tage, S. E., Garnett, M. H., Jones, T. G., Freeman, C., Hooijer, A., Wiltshire, A. J., S.H.Limin, and Gauci, V.: Deep instability of deforsted tropical peatlands revealed by fluvial organic carbon fluxes, *Nature*, 493, 660–663, <https://doi.org/10.1038/nature11818>, 2013.
- Müller, D., Warneke, T., Rixen, T., Müller, M., Jamahari, S., Denis, N., Mujahid, A., and Notholt, J.: Lateral carbon fluxes and CO₂ outgassing from a tropical peat-draining river, *Biogeosciences*, 12, 5967–5979, <https://doi.org/10.5194/bg-12-5967-2015>, 2015.
- Müller, D., Warneke, T., Rixen, T., Müller, M., Mujahid, A., Bange, H., and Notholt, J.: Fate of peat-derived carbon and associated CO₂ and CO emissions from two Southeast Asian estuaries, *Biogeosciences*, <https://doi.org/10.5194/bgd-12-8299-2015>, 2016.
- Müller-Dum, D., Warneke, T., Rixen, T., Müller, M., Christodoulou, A., Baum, A., Oakes, J., Eyre, B. D., and Notholt, J.: Impact of peatlands on carbon dioxide (CO₂) emissions from the Rajang River and Estuary, Malaysia, *Biogeosciences*, 16, 17–32, <https://doi.org/10.5194/bg-2018-391>, 2018.
- Page, S. E., Rieley, J. O., and Banks, C. J.: Global and regional importance of the tropical peatland carbon pool, *Global Change Biology*, 17, 798–818, <https://doi.org/10.1111/j.1365-2486.2010.02279.x>, 2011.
- Pereira, M., Amaro, A., Pintado, M., and Poças, M.: Modeling the effect of oxygen pressure and temperature on respiration rate of ready-to-eat rocket leaves. A probabilistic study of the Michaelis-Menten model, *Postharvest Biology and Technology*, 131, 1 – 9, <https://doi.org/10.1016/j.postharvbio.2017.04.006>, 2017.
- Pind, A., Freeman, C., and Lock, M. A.: Enzymic degradation phenolic materials in peatlands, *Plant and Soil*, 159, 227–231, <https://doi.org/10.1007/BF00009285>, 1994.
- Raymond, P. A., Zappa, C. J., Butman, D., Bott, T. L., Potter, J., Mulholland, P., Laursen, A. E., McDowell, W. H., and Newbold, D.: Scaling the gas transfer velocity and hydraulic geometry in streams and small rivers, *Limnology and Oceanography: Fluids and Environments*, 2, 41–53, <https://doi.org/10.1215/21573689-1597669>, 2012.
- Raymond, P. A., Hartmann, J., Sobek, S., Hoover, M., McDonald, C., Butman, D., Striegel, R., Mayorga, E., Humborg, C., Kortelainen, P., Dürr, H., Meybeck, M., Ciais, P., and Guth, P.: Global carbon dioxide emissions from inland waters, *Nature*, 503, 355–359, <https://doi.org/10.1038/nature12760>, 2013.
- Regnier, P., Friedlingstein, P., Ciais, P., Mackenzie, F. T., Gruber, N., Janssens, I. A., Laruelle, G. G., Lauerwald, R., Luyssaert, S., Andersson, A. J., Arndt, S., Arnosti, C., Borges, A. V., Dale, A. W., Gallego-Sala, A., Goddérís, Y., Goossens, N., Hartmann, J., Heinze, C., Ilyina, T., Joos, F., LaRowe, D. E., Leifeld, J., Meysman, F. J. R., Munhoven, G., Raymond, P. A., Spahni, R., Suntharalingam, P., and Thullner, M.:



- 370 Anthropogenic perturbation of the carbon fluxes from land to ocean, *Nature Geoscience*, 6, 597–607, <https://doi.org/10.1038/ngeo1830>, 2013.
- Rixen, T., Baum, A., Pohlmann, T., Blazer, W., Samiaji, J., and Jose, C.: The Siak, a tropical black water river in central Sumatra on the verge of anoxia, *Biogeochemistry*, 90, 129–140, <https://doi.org/10.1007/s10533-008-9239-y>, 2008.
- Rixen, T., Baum, A., Wit, F., and Samiaji, J.: Carbon leaching from tropical peat soils and consequences for carbon balances, *Frontiers in Earth Science*, 4, 74, <https://doi.org/10.3389/feart.2016.00074>, 2016.
- 375 Sinsabaugh, R.: Phenol oxidase, peroxidase and organic matter dynamics of soil, *Soil Biology and Biochemistry*, 42, 391–404, <https://doi.org/10.1016/j.soilbio.2009.10.014>, 2010.
- Sinsabaugh, R. L., Lauber, C. L., Weintraub, M. N., Ahmed, B., Allison, S. D., Crenshaw, C., Contosta, A. R., Cusack, D., Frey, S., Gallo, M. E., Gartner, T. B., Hobbie, S. E., Holland, K., Keeler, B. L., Powers, J. S., Stursova, M., Takacs-Vesbach, C., Waldrop, M. P., Wal-
- 380 lenstein, M. D., Zak, D. R., and Zeglin, L. H.: Stoichiometry of soil enzyme activity at global scale, *Ecology Letters*, 11, 1252–1264, <https://doi.org/https://doi.org/10.1111/j.1461-0248.2008.01245.x>, 2008.
- Taylor, L. L., Quirk, J., Thorley, R. M. S., Kharecha, P. A., Hansen, J., Ridgwell, A., Lomas, M. R., Banwart, S. A., and Beerling, D. J.: Enhanced weathering strategies for stabilizing climate and averting ocean acidification, *Nature Climate Change*, 6, 1758–6798, <https://doi.org/10.1038/nclimate2882>, 2016.
- 385 Vaquer-Sunyer, R. and Duarte, C. M.: Thresholds of hypoxia for marine biodiversity, *PNAS*, <https://doi.org/10.1073/pnas.0803833105>, 2008.
- Wanninkhof, R.: Relationship between wind speed and gas exchange over the ocean, *Journal of Geophysical Research: Oceans*, 97, 7373–7382, <https://doi.org/10.1029/92JC00188>, 1992.
- Weiss, R.: The solubility of nitrogen, oxygen and argon in water and seawater, *Deep Sea Research and Oceanographic Abstracts*, 17, 721 – 735, [https://doi.org/https://doi.org/10.1016/0011-7471\(70\)90037-9](https://doi.org/https://doi.org/10.1016/0011-7471(70)90037-9), <http://www.sciencedirect.com/science/article/pii/0011747170900379>,
- 390 1970.
- Weiss, R. F.: Carbon dioxide in water and seawater: The solubility of a non-ideal gas, *Marine Chemistry*, 2, 203–215, [https://doi.org/10.1016/0304-4203\(74\)90015-2](https://doi.org/10.1016/0304-4203(74)90015-2), 1974.
- Williams, C. J., Shingara, E. A., and Yavitt, J. B.: Phenol oxidase activity in peatlands in new york state: Response to summer drought and peat type, *Wetlands*, 20, 416–421, [https://doi.org/10.1672/0277-5212\(2000\)020\[0416:POAIP\]2.0.CO;2](https://doi.org/10.1672/0277-5212(2000)020[0416:POAIP]2.0.CO;2), 2000.
- 395 Wit, F., Müller, D., Baum, A., Warneke, T., Pranowo, W. S., and Müller, M.: The impact of disturbed peatlands on river outgassing in Southeast Asia, *Nature Communications*, 6, <https://doi.org/10.1038/ncomms10155>, 2015.
- Wit, F., Rixen, T., Baum, A., Pranowo, W. S., and Hutahaean, A. A.: The Invisible Carbon Footprint as a hidden impact of peatland degradation inducing marine carbonate dissolution in Sumatra, Indonesia, *Scientific Reports*, 8, 2045–2322, <https://doi.org/10.1038/s41598-018-35769-7>, 2018.
- 400 Yatagai, A., Maeda, M., Khadgarai, S., Masuda, M., and Xie, P.: End of the Day (EOD) Judgment for Daily Rain-Gauge Data, *journal = Atmosphere*, DOI = 10.3390/atmos11080772., 2020.